

SCIENTIFIC REPORTS



OPEN

TMED3 promotes hepatocellular carcinoma progression via IL-11/STAT3 signaling

Hao Zheng^{1,*}, Yuan Yang^{1,2,*}, Jun Han^{1,3,*}, Wei-hua Jiang⁴, Cheng Chen⁵, Meng-chao Wang¹, Rong Gao³, Shuai Li⁶, Tao Tian¹, Jian Wang¹, Li-jun Ma⁴, Hao Ren³ & Wei-ping Zhou¹

Received: 27 May 2016
Accepted: 24 October 2016
Published: 30 November 2016

Transmembrane p24 trafficking protein 3 (TMED3) is a metastatic suppressor in colon cancer, but its function in the progression of hepatocellular carcinoma (HCC) is unknown. Here, we report that TMED3 was up-regulated in HCC and portal vein tumor thrombus. TMED3 up-regulation in HCC was significantly correlated with aggressive characteristics and predicted poor prognosis in HCC patients. TMED3 overexpression in HCC cell lines promoted cell migration and invasion. In contrast, TMED3 knockdown suppressed HCC metastasis both *in vitro* and *in vivo*. Gene microarray analysis revealed decreased IL-11 expression in TMED3-knockdown cells. We propose that TMED3 promotes HCC metastasis through IL-11/STAT3 signaling. Taken together, these findings demonstrate that TMED3 promotes HCC metastasis and is a potential prognostic biomarker in HCC.

Hepatocellular carcinoma (HCC) is one of the most lethal malignancies^{1–3}. With improvements in surgical techniques and perioperative management, the five-year survival rates for HCC after curative therapy have somewhat increased^{2,4,5}. However, the rates of recurrence and intrahepatic or extrahepatic metastasis after surgery remain high^{6–8}, thus limiting the prognosis for HCC patients^{9,10}. Therefore, a comprehensive understanding of the molecular pathogenesis of HCC recurrence and metastasis is imperative.

The transmembrane emp24 domain-containing protein (TMED)/p24 family is involved in the vesicular trafficking of proteins and innate immune signaling. The ten mammalian family members, which are conserved across species, are separated into four subfamilies (α , β , δ , γ)¹¹. TMED proteins primarily exist as monomers, dimers, oligomers and hetero-oligomers in eukaryotes^{12–14}. These proteins contain a GOLD (Golgi dynamics) domain, which is a β -strand-rich domain found in several proteins that are involved in Golgi dynamics and intracellular protein trafficking^{13,15}. Many TMED proteins have been investigated and reported on in detail^{16,17}. TMED7, which negatively regulates TLR4 signaling, was identified as a specific inhibitor of the MyD88-independent TLR4 signaling pathway through its ability to facilitate the disruption of the TRIF/TRAM complex by TAG^{18–20}. However, the clinical significance of TMED3 and its role in HCC pathogenesis remain unknown.

In the present study, we demonstrate that TMED3 was up-regulated in HCC tissues and was expressed at even higher levels in portal vein tumor thrombus (PVTT). TMED3 up-regulation was associated with poor clinical outcome in HCC patients. TMED3 down-regulation dramatically attenuated HCC migration both *in vitro* and *in vivo*. A gene microarray analysis of a TMED3-knockdown cell line revealed low IL-11 expression. These findings suggest that TMED3 plays an important role in HCC progression through IL-11/STAT3 signaling and may be useful for future HCC therapy.

¹The Third Department of Hepatic Surgery, Eastern Hepatobiliary Surgery Hospital, Second Military Medical University, 225 Changhai Road, Shanghai 200438, China. ²Department of Health Statistics, Second Military Medical University, 800 Xiangyin Road, Shanghai 200433, China. ³Department of Microbiology, Shanghai Key Laboratory of Medical Biodefense, Second Military Medical University, 800 Xiangyin Road, Shanghai 200433, China. ⁴Department of Oncology, Shanghai Tongren Hospital, Shanghai Jiaotong University, 1111 Xianxia Road, Shanghai 200336, China. ⁵Department of Medical Oncology, Jinling Hospital, 305 Zhongshan East Road, Nanjing, Jiangsu 210000, China. ⁶Department of Computer Science, Rensselaer Polytechnic Institute, 110 8th Street, Troy, NY, 12180, United States. *These authors contributed equally to this work. Correspondence and requests for materials should be addressed to L.-j.M. (email: lijun.ma@shtrhospital.com) or H.R. (email: hren2013@139.com) or W.-P.Z. (email: ehphwp@126.com)

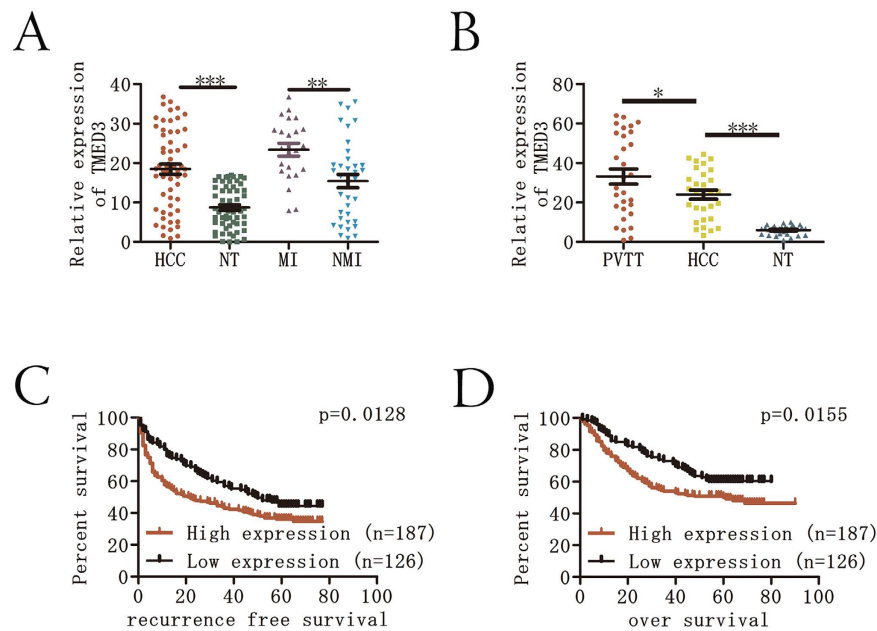


Figure 1. TMED3 expression is up-regulated in HCC and in cases of PVTT. (A) Relative TMED3 mRNA expression levels in 60 cases of HCC, including 25 MI and 35 NMI, were analyzed by RT-PCR and normalized to β -actin. (B) Relative TMED3 mRNA expression levels in 30 cases of HCC with PVTT were analyzed by RT-PCR and normalized to β -actin. (C) The high TMED3 expression group had a shorter RFS than the low TMED3 expression group. (D) The high TMED3 expression group had a shorter OS than the low TMED3 expression group. * $p < 0.05$, ** $p < 0.01$, *** $p < 0.001$.

Results

TMED3 expression is up-regulated in HCC and PVTT. To clarify the underlying role of TMED3 in HCC progression, we performed qRT-PCR analysis of 60 HCC specimens and paired non-tumor (NT) samples. TMED3 mRNA levels were significantly up-regulated in most HCC tissues (Fig. 1A). We next examined TMED3 protein levels by immunohistochemistry (IHC) on a tissue microarray containing 313 paired HCC tissues. Immunostaining revealed that 63.9% (200/313) of the HCC tissues showed higher TMED3 protein levels than their corresponding adjacent noncancerous tissues (Fig. S1B and C). To further investigate the role of TMED3 in HCC metastasis, we examined TMED3 expression in primary metastatic or non-metastatic HCC. TMED3 expression was higher in metastasis-inclined (MI) HCC than in non-metastasis-inclined (NMI) HCC (Fig. 1A). Furthermore, we examined TMED3 expression in 30 matched PVTT, primary tumor and NT tissues. Intriguingly, TMED3 mRNA levels were significantly higher in PVTT than in primary tumors or NT tissues (Fig. 1B), suggesting that TMED3 may play a role in HCC metastasis. To investigate the clinical significance of TMED3 in HCC, the cohort of 313 HCC patients was divided into two groups according to the tumor IHC score: a high TMED3 expression group (tumor score > 2 , $n = 187$) and a low TMED3 expression group (tumor score ≤ 2 , $n = 126$). High TMED3 expression was associated with positive alpha-fetoprotein (AFP; $P = 0.020$), larger tumor size (≥ 5 cm; $P = 0.045$) and vascular invasion ($P < 0.001$) (Table 1). Kaplan–Meier analysis revealed that patients in the high TMED3 expression group exhibited worse relapse-free survival (RFS) and overall survival (OS) than patients in the low expression group ($P = 0.0128$ and $P = 0.0155$, respectively) (Fig. 1C and D). A univariate analysis indicated that among the clinicopathological characteristics, TMED3 expression level, tumor size, vascular invasion, and positivity for AFP, HBeAg, or HBeAg were correlated with RFS, and TMED3 expression level, tumor size, tumor number, AFP positivity, vascular invasion, presence of HBsAg, and presence of HBeAg were correlated with OS (Table 2). Furthermore, multivariate Cox regression analysis indicated that TMED3 expression level, tumor size, presence of HBeAg, and presence of HBsAg were independent risk factors for RFS, and TMED3 expression level, tumor size, tumor number, and presence of HBsAg were independent risk factors for OS in HCC patients (Table 3). These results indicated that TMED3 could be used as a prognostic biomarker for HCC.

TMED3 promotes HCC cell metastasis *in vitro*. To explore the biological functions of TMED3 in HCC *in vitro*, we first detected TMED3 expression in a normal human liver cell line (HL7702) and in HCC cell lines with varying metastatic potential (HCCLM3, MHCC97H, MHCC97L, SMMC-7721, Huh7, HepG2, Hep3B). TMED3 expression levels were higher in the highly metastatic HCC cell lines (HCCLM3, MHCC97H) than in the less metastatic cell lines (SMMC-7721, MHCC97L); the normal liver cell line had the lowest TMED3 expression (Fig. S2A). Two HCC cell lines (HepG2, Huh7) with median TMED3 expression were selected to establish TMED3-knockdown or TMED3-overexpressing cells. TMED3 expression was validated by qRT-PCR (Fig. S2B and C). A wound healing migration assay showed that TMED3 knockdown inhibited cell migration, whereas TMED3 overexpression enhanced cell mobility (Fig. 2A and C). A transwell invasion assay revealed

	TMED3 ^a		χ^2	P value
	High	Low		
All cases				
Age, y			0.001	0.981
≥55	70	47		
<55	117	79		
Gender			0.340	0.854
Male	166	111		
Female	21	15		
HBsAg			2.358	0.125
Positive	167	105		
Negative	20	21		
HBeAg			0.527	0.468
Positive	42	24		
Negative	145	102		
AFP, μg/L			5.384	0.020
≥20	128	70		
<20	59	56		
Tumor size, cm			4.013	0.045
≥5	112	61		
<5	75	65		
Tumor number			0.011	0.917
Single	149	101		
Multiple	38	25		
Vascular invasion			62.822	<0.001
Present	146	42		
Absent	41	84		
Tumor differentiation			2.393	0.122
I–II	16	18		
III–IV	168	108		

Table 1. Clinical characteristics of 313 HCC patients according to TMED3 expression level. Values in red are statistically significant ($P < 0.05$). AFP, alpha-fetoprotein; HBsAg, hepatitis B surface antigen; HBeAg, hepatitis B e antigen. ^aPatients whose tumor tissue immunohistochemistry score was >2 were included in the high expression group, and the remaining patients comprised the low expression group.

Variate	Recurrence Free Survival		Overall Survival	
	Hazard ratio	P value	Hazard ratio	P value
TMED3 (High expression)	1.520 (1.127–2.049)	0.006	1.547 (1.099–2.178)	0.012
Tumor size (>5 cm)	1.449 (1.081–1.941)	0.013	1.861 (1.323–2.616)	<0.001
Tumor number (Multiple)			1.583 (1.090–2.300)	0.016
AFP (positive)	1.503 (1.107–2.042)	0.009	1.453 (1.026–2.056)	0.035
HBeAg (positive)	2.012 (1.204–3.361)	0.008	2.130 (1.152–3.940)	0.016
HBsAg (positive)	1.548 (1.116–2.146)	0.009	1.499 (1.042–2.158)	0.029
Vascular invasion	1.580 (1.168–2.136)	0.003	1.547(1.116–2.220)	0.010

Table 2. Univariate analysis of the risk factors for HCC recurrence and overall survival.

that TMED3-knockdown cells displayed impaired migration, whereas cells overexpressing TMED3 exhibited increased invasiveness (Fig. 2B and D). These results indicated that TMED3 promotes HCC metastasis *in vitro*.

TMED3 promotes HCC metastasis *in vivo*. To verify the function of TMED3 *in vivo*, we injected luciferase-expressing HepG2-siTMED3 and HepG2-GFP cells into the lateral tail vein of mice to establish a lung metastasis model. The process of lung metastasis was dynamically monitored every week using an *in vivo* imaging system. Bioluminescent imaging revealed that TMED3 knockdown suppressed HCC lung metastasis (Fig. 3A and C). After 42 days, the lungs were dissected and stained with hematoxylin and eosin (H&E). Fewer micrometastases were microscopically detected in the lungs of mice in the TMED3-knockdown group (Fig. 3B and D). Additionally, we injected HepG2-siTMED3 and HepG2-GFP cells subcutaneously into nude mice. Weekly tumor volume measurements showed that TMED3 had no effect on cell growth (Fig. S3A and B). These data demonstrated that TMED3 may promote the metastasis of hepatoma cells *in vivo*.

Variable	Recurrence-free Survival		Overall Survival	
	Hazard ratio	P value	Hazard ratio	P value
TMED3 (high expression)	1.403 (1.038–1.898)	0.028	1.446 (1.025–2.040)	0.035
Tumor size (>5 cm)	1.503 (1.118–2.020)	0.007	1.841 (1.306–2.594)	<0.001
Tumor number (Multiple)			1.587 (1.091–2.308)	0.016
HBeAg (positive)	1.523 (1.095–2.118)	0.012		
HBsAg (positive)	2.016 (1.204–3.374)	0.008	2.322 (1.251–4.310)	0.008

Table 3. Multivariate analysis of risk factors for HCC recurrence and overall survival.

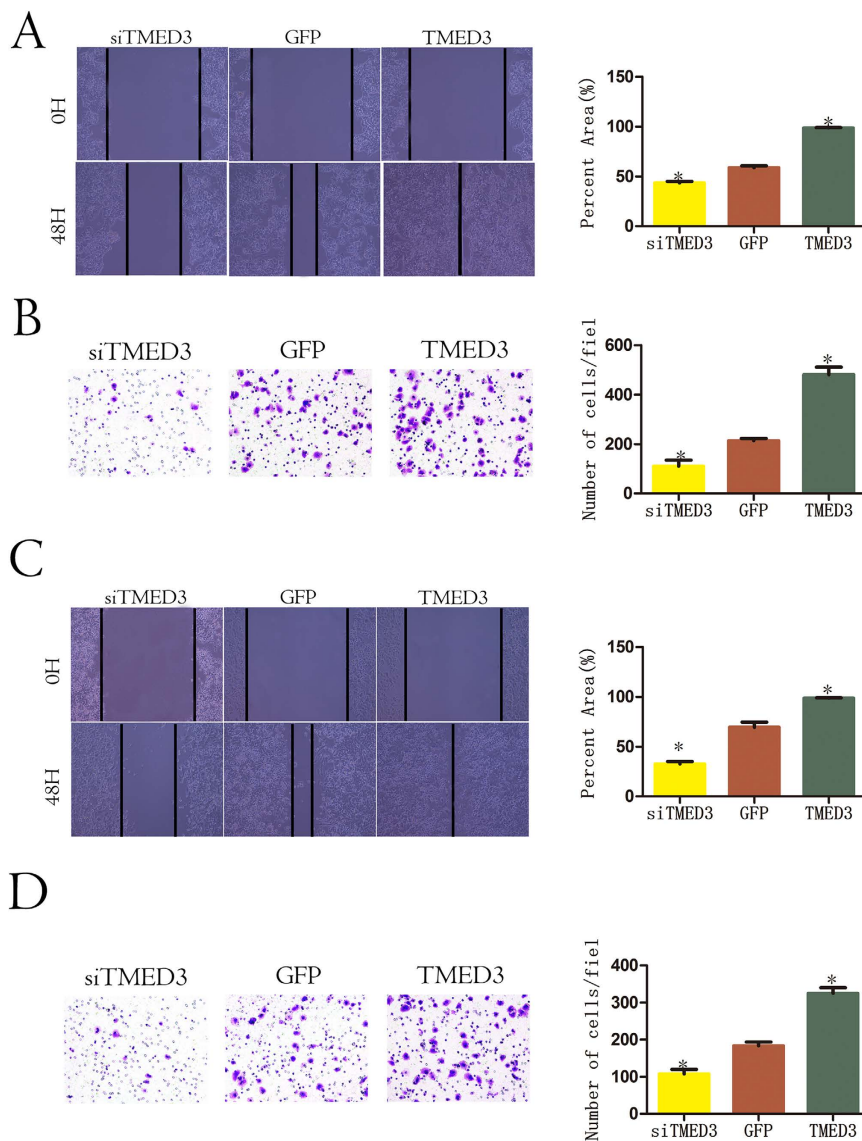


Figure 2. TMED3 promotes HCC metastasis *in vitro*. Wound healing and transwell migration assays showed that TMED3 knockdown inhibits migratory properties and that TMED3 overexpression promotes migration in the HCC-derived cell lines HepG2 (A,B) and Huh7 (C,D). Representative results and a statistical analysis are shown. (A–D) $n = 3$, mean \pm SD. The Student's t test, * $p < 0.05$ versus GFP control.

TMED3 promotes cell migration by increasing IL-11 expression. To explore the molecular mechanism of TMED3 in HCC cell metastasis, gene microarray analysis was utilized to compare the expression profiles of TMED3-knockdown and control HCC cells. A total of 64 genes were significantly up-regulated, and 95 genes were down-regulated (>1.5 -fold, siTMED3/GFP). Interleukin 11 (IL-11), which has been reported to regulate metastasis and cell adherence^{21,22}, was the most robustly down-regulated gene in HepG2-siTMED3 cells

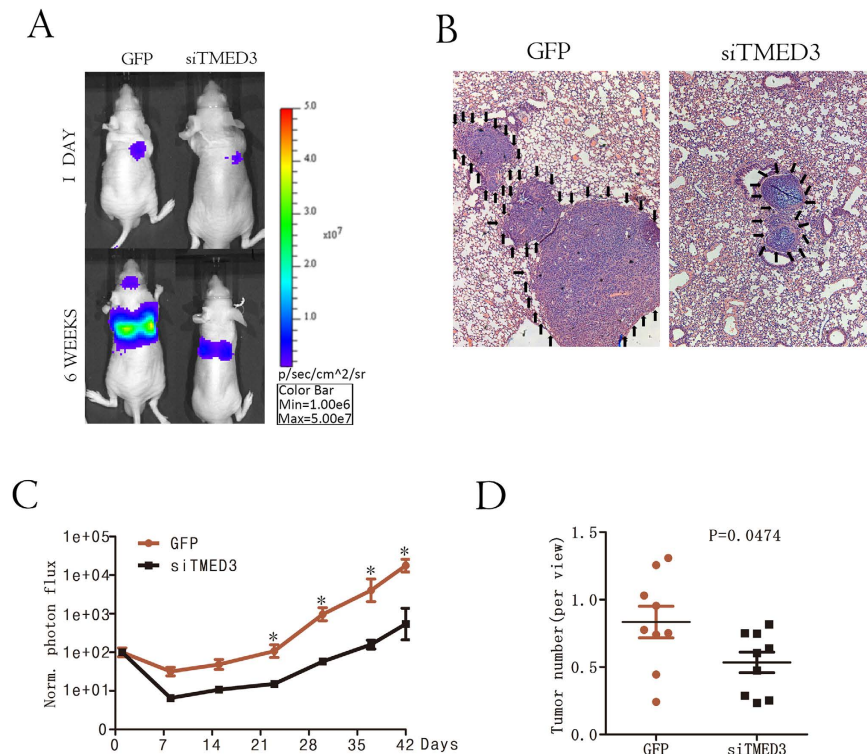


Figure 3. TMED3 promotes HCC metastasis *in vivo*. (A) Lung metastases that developed after injecting HepG2 cell lines in the lateral tail vein were imaged using the IVIS Imaging System. Representative luciferase signals captured in each group ($n = 9$) at initial injection and after 42 days are shown. The statistical analysis is shown in (C), $n = 9$, mean \pm SD, the Student's *t* test, * $p < 0.05$ versus GFP control. (B) Representative imaged of H&E-stained lung metastatic loci from each group in (A). The statistical analysis is shown in (D).

(Fig. 4A). Western blotting validated IL-11 up-regulation in cells overexpressing TMED3 and down-regulation in TMED3-knock down cells (Fig. 4B and C). To examine whether TMED3 increases IL-11 secretion, we measured IL-11 levels in the supernatant from different cell clones. TMED3 overexpression increased IL-11 levels in the supernatant, and TMED3 knockdown reduced IL-11 levels in the supernatant (Fig. 4D and E). These results indicated that TMED3 up-regulates IL-11 expression, leading to increased IL-11 secretion. As Signal transducer and activator of transcription 3 (STAT3) is the main signaling molecule downstream of IL-11, we also measured STAT3 phosphorylation levels. TMED3 overexpression led to increased STAT3 phosphorylation, and TMED3 knockdown decreased STAT3 activation (Fig. 4F and G). Importantly, a strong positive correlation between TMED3 and STAT3 phosphorylation levels was observed in clinical samples (Fig. S4). This finding suggested that TMED3 may promote metastasis at least partially through IL-11/STAT3 signaling.

Discussion

Despite the available advanced surgical and medical treatments^{1,2}, HCC recurrence and metastasis rates remain high due to the long-term interactions between environmental and genetic factors²³, and the prognosis of HCC patients is still unsatisfactory^{24–26}. Although multiple tumor suppressor genes and oncogenes involved in HCC have been identified^{27–31}, our knowledge of the underlying cellular and molecular pathways in HCC progression remains limited. The molecular markers that effectively define the risk of HCC recurrence need to be identified and characterized to predict patient outcome and determine optimal medical management strategies.

In a previous study, TMED3 was found to be a metastatic suppressor in colon cancer³², but the function of TMED3 in HCC progression was unknown. In this study, we explored the clinical significance and role of TMED3 in HCC progression by measuring TMED3 protein levels in a large cohort of 313 patients. TMED3 up-regulation correlated with a high AFP level ($P = 0.020$), tumor size ($P = 0.045$) and vascular invasion ($P < 0.001$). Kaplan–Meier analysis revealed that patients with higher TMED3 expression had higher recurrence rates ($P = 0.0128$) and shorter survival times after curative resection ($P = 0.0155$), indicating that TMED3 expression is associated with HCC progression and may serve as an independent prognostic marker of HCC patient survival. To further investigate the effects of TMED3 in HCC cells, we performed gain- and loss-of-function experiments. Our data showed that TMED3 down-regulation suppressed HCC migration and invasion *in vitro* and lung metastasis *in vivo*. Thus, TMED3 can functionally promote HCC cell metastasis.

IL-11 belongs to the IL-6 family^{33,34}, and similar to most cytokines in this family, IL-11 is produced by various cells in response to inflammatory stimulators. IL-11 exhibits a wide variety of biological effects in the hematopoietic and immune systems^{35–37}. It has been reported that IL-11 promotes the development of gastric, breast, and colorectal cancer and contributes to the bone metastasis of HCC^{38–40}. STAT proteins are potent, conserved

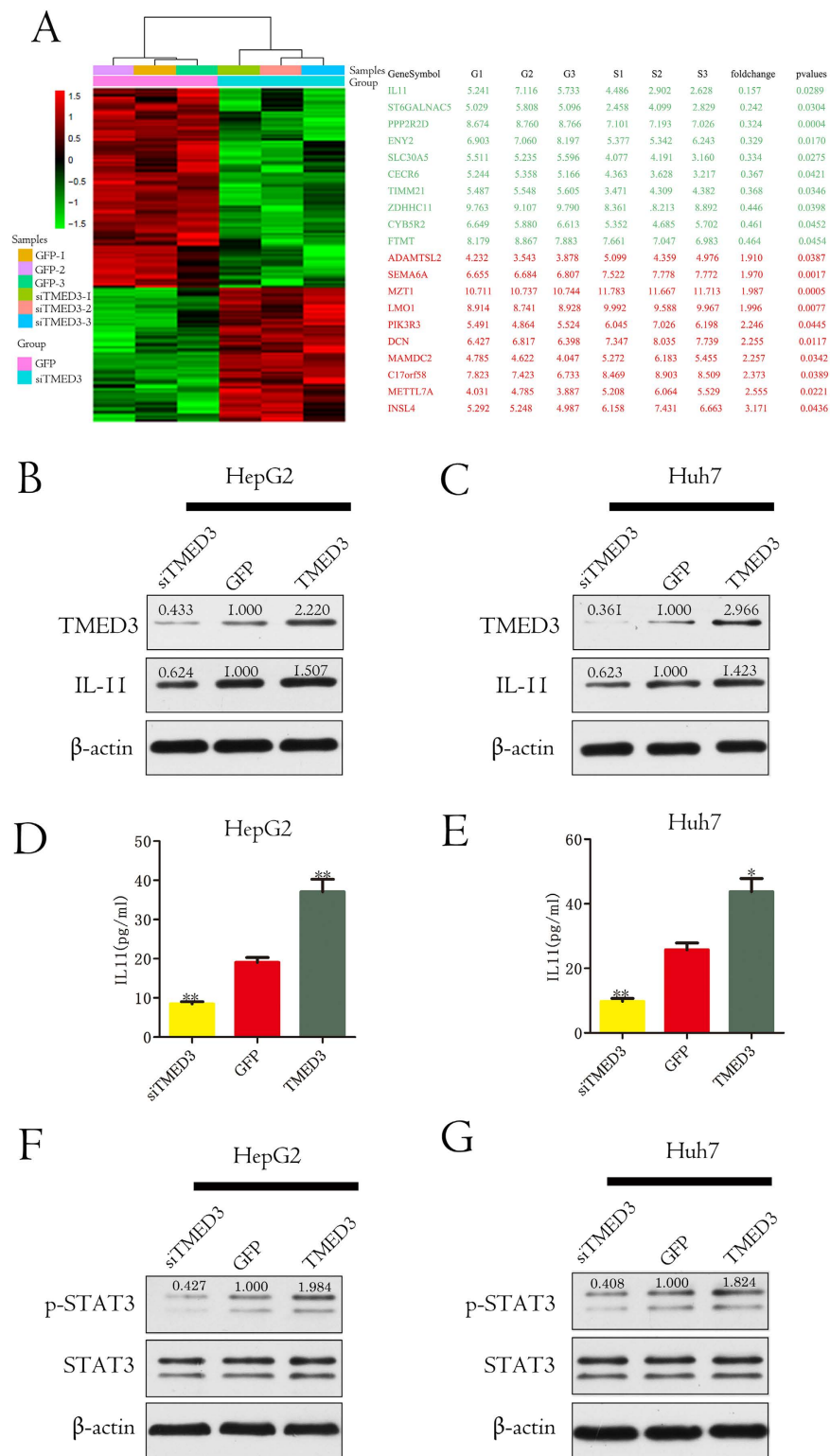


Figure 4. TMED3 promotes cell migration by increasing IL-11 expression. (A) Differentially expressed genes in HepG2-siTMED3 cells compared with control cells. The top 10 up- and down-regulated genes are listed on the right. (B,C) Relative IL-11 expression in cells with stable TMED3 knockdown or overexpression and paired controls. IL-11 expression was analyzed by western blot and normalized to β -actin. (D,E) The IL-11 concentration in culture medium from cells with stable TMED3 knockdown or overexpression and paired controls was determined by ELISA. $n = 3$, mean \pm SD, the Student's t test, $*p < 0.05$ versus GFP control, $**p < 0.01$ versus GFP control. (F,G) Relative P-STAT3 and STAT3 expression levels in cells with stable TMED3 knockdown or overexpression and paired controls were analyzed by western blot and normalized to β -actin. (B-G) $n = 3$.

transcription factors. Seven STAT proteins have been identified as latent cytoplasmic transcription factors activated by tyrosine phosphorylation in response to cytokine and growth factor stimulation^{41,42}. STAT signaling plays an important role in the transfer of extracellular signals into the nucleus, resulting in transcriptional regulation, and is essential in the uncontrolled growth of cancer cells, angiogenesis and metastasis^{43,44}. In our gene microarray analysis, we observed decreased IL-11 expression in TMED3-knockdown cells. Moreover, STAT3 activation correlated with TMED3 expression. These results suggested that TMED3 may promote HCC metastasis through IL-11/STAT3 signaling. However, the relationship between TMED3 and IL-11 remains unclear and requires further investigation.

In conclusion, our study determined that TMED3 is a valuable prognostic biomarker for HCC and revealed the role and potential mechanism of action of TMED3 in HCC metastasis. A complete understanding of TMED3 function and mechanism of action will reveal novel strategies for HCC treatment.

Materials and Methods

Ethics statement. All the clinical specimens were obtained with informed consent and approved by the Clinical Research Ethics Committee of Eastern Hepatobiliary Surgery Hospital, Informed consent was obtained from all patients involved in this study. Animal experiments were reviewed and approved by the Institutional Animal Care and Use Committee of the Second Military Medical University. All the experiments were performed in accordance with the approved guidelines of the Institutional Research Ethics Committee of the Second Military Medical University University.

Patients and specimens. This study included 60 HCC tissues and paired NT tissues (including 25 MI and 35 NMI) which were obtained from the Eastern Hepatobiliary Surgery Hospital for qRT-PCR analysis and these tissues were aimed to investigate the mRNA level of TMED3 and the clinicopathologic characteristic was shown in supplement Table 1. The MI group was composed of patients with solitary HCC that was accompanied by either portal vein metastasis or venous metastases at follow-up. The NMI group was restricted to only those patients with solitary HCC and no recurrence at follow-up. For further confirmation that TMED3 may be associated with tumor metastasis, other samples from 30 patients with HCC and PVTT were used to evaluate TMED3 expression levels in paired HCC/NT/PVTT samples by qRT-PCR. The clinicopathologic characteristic was shown in supplement Table 2. To study the correlation of TMED3 with clinical characteristics and prognosis, a large cohort of 313 patients with HCC (randomly collected from January 2006 to September 2010) who received high-quality follow-up was used to examine TMED3 protein levels by tissue microarray (TMA) and IHC and to ascertain the clinical significance of TMED3. The clinicopathologic characteristics were shown in Table 1. All HCC specimens were obtained immediately after hepatectomy. Tissues were then fixed in 10% buffered formalin and embedded in paraffin. The fresh specimens used in this study were snap-frozen from tissues prior to formalin fixation, transferred to liquid nitrogen, and stored at -80°C .

Tissue microarray construction and immunohistochemical analysis. Briefly, all samples from patients in the HCC cohort were reviewed histologically after H&E staining. Representative areas distant from necrotic and hemorrhagic tissue were marked on the paraffin blocks. Two 1.0-mm cores were extracted from each tumor, paired with NT tissue and mounted on a new recipient block using a semi-automated arraying device (TMArrayer, Pathology Devices, Westminster, MD, USA). IHC was performed on the TMA using a two-step immunoperoxidase technique. A TMED3 polyclonal antibody (Abcam, CA, USA) diluted 1:60 was used as the primary antibody. Briefly, after heating the sections in 10 mmol/l citrate buffer for antigen retrieval, the sections were incubated first with the primary antibody and then with the secondary antibody for one hour at room temperature. Finally, the sections were developed in diaminobenzidine solution under a microscope and counter-stained with hematoxylin. The IHC stains were assessed by three separate observers who had no knowledge of patient characteristics. TMED3 staining was abundant in the cytoplasm and nucleus. The expression was recorded after evaluating the staining intensity of positive cells (0 = none; 1 = + weak; 2 = ++ intermediate; 3 = +++ strong; 4 = ++++ very strong), as shown in Fig. S1A.

RNA extraction, cDNA preparation and quantitative real-time PCR (qRT-PCR). Total RNA was extracted from snap-frozen tissues using TRIzol reagent (Takara, Dalian, China) according to the manufacturer's instructions. The quality of the total RNA was assessed using a Nanodrop 2000 and via agarose gel electrophoresis. First-strand cDNA was synthesized from 1–2 μg of total RNA using random primers and M-MLV Reverse Transcriptase (Invitrogen, CA). Real-time PCR was performed according to the SYBR Green protocol in a Step One Plus System (Applied Biosystems, Foster City, CA) with β -actin as the endogenous control. The TMED3-specific primers were 5'-GGGTCTCTGTACCTGAGGAAA-3' (forward) and 5'-CACCCAGGGTGAGCAGAT-3' (reverse), and the β -actin-specific primers were 5'-TGACGTGGACATCCGCAAAG-3' (forward) and 5'-CTGGAAGGTGGACAGCGAGG-3' (reverse). The relative mRNA levels were calculated based on the Ct values and were normalized to β -actin expression.

Cell culture. Human HCC cell lines were purchased from the Shanghai Institute of Life Sciences Cell Resource Center (Shanghai, China). All cell lines were cultured in Dulbecco's Modified Eagle Medium (DMEM, HyClone, CA, USA) supplemented with 10% fetal bovine serum (FBS) and 1% penicillin/streptomycin (Gibco, CA, USA). All cell cultures were maintained at 37°C in a humidified atmosphere with 5% CO_2 .

Wound healing assays. For the wound healing assays, monolayer cells plated in 12-well plates were wounded with a plastic 200- μl pipette tip and then rinsed several times with medium to remove floating cells. The wound healing process was monitored using an inverted light microscope (Olympus).

Western blot analysis. Total cell and tissue lysates were prepared in $1\times$ sodium dodecyl sulfate buffer. Identical quantities of proteins were separated by sodium dodecyl sulfate-polyacrylamide gel electrophoresis and transferred onto nitrocellulose filter membranes. After incubation with antibodies specific for TMED3 (ab151056, ab173112; Abcam, CA, USA), IL-11 (ab187167; Abcam, CA, USA), STAT3 (ab119352; Abcam, CA, USA), P-STAT3 (ab76315; Abcam, CA, USA) or β -actin (ab8226; Abcam, CA, USA), the blots were incubated with IRDye 800-conjugated goat anti-rabbit IgG and IRDye 700-conjugated goat anti-mouse IgG, and the bands were detected using an Odyssey infrared scanner (Li-Cor). β -Actin was used as a loading control.

Wound healing migration assay. Briefly, 1×10^5 cells/well were plated in 6-well plates. After the cells attached, a wound was created in the middle of each well, and the medium was replaced with serum-free medium. The area of healing across the lesion was measured after a 48-h incubation.

Transwell assays. Millicell 24-well culture insert plates (Millipore, USA) and polycarbonate membranes with a pore size of $8\mu\text{m}$ were used for transwell assays. First, the insert plates were equilibrated with 0.5 ml of DMEM for 1 h at 37°C in 5% CO_2 ; then, the medium in the lower chambers was replaced with 0.5 ml of DMEM supplemented with 10% FBS. In total, 50,000 cells in $400\mu\text{l}$ of serum-free DMEM were loaded into the upper chambers. After a 24-h incubation, the inserts were rinsed with PBS, and the upper surfaces of the membranes were scraped to remove the cells. The cells on the underside of the membrane were stained with Giemsa stain and counted under a microscope. Cells from each culture condition were examined in quadruplicate.

Animal studies. To explore the effects of TMED3 on tumor growth *in vivo*, 1×10^7 HepG2 cells that stably knocked down TMED3 and control cells were subcutaneously implanted into the bilateral armpit of nine BALB/C nude mice. The tumor volumes were measured every week after implantation (volume $V = \text{length} \times \text{width} \times \text{length} \times 1/2$). All mice were sacrificed five weeks later. A tail vein injection model was also used to evaluate the potential of the cells to metastasize to the lungs. The metastases were monitored using an IVIS@ Lumina II system (Caliper Life Sciences, Hopkinton, MA) for 10 min after intraperitoneal injection of 4.0 mg of luciferin (Gold Biotech) in $50\mu\text{l}$ of saline. Animals were housed in cages under standard conditions, and the methods were carried out following the requirements of the Second Military Medical University Animal Care Facility and the National Institutes of Health guidelines, and all experimental protocols were approved by the Institutional Animal Care and Use Committee of the Second Military Medical University, Shanghai, China. The mice were kept in pathogen-free conditions.

Gene expression profiling and analysis. Total RNA was extracted using TRIzol Reagent (Life Technologies, Carlsbad, CA, US) according to the manufacturer's instructions, and the RNA integrity number (RIN) was determined using an Agilent Bioanalyzer 2100 (Agilent Technologies, Santa Clara, CA, US). Acceptable total RNA preparations were further purified using an RNeasy Mini Kit (QIAGEN, GmbH, Germany) and RNase-Free DNase (QIAGEN, GmbH, Germany). Total RNA was amplified and labeled using a Low Input Quick Amp Labeling Kit, One-Color (Agilent Technologies, Santa Clara, CA, US) according to the manufacturer's instructions. Labeled cRNA was purified using an RNeasy Mini Kit (QIAGEN, GmbH, Germany). Each slide was hybridized with $1.65\mu\text{g}$ of Cy3-labeled cRNA in a hybridization oven using the Gene Expression Hybridization Kit (Agilent Technologies, Santa Clara, CA, US) according to the manufacturer's instructions. After 17 h of hybridization, slides were washed in staining dishes (Thermo Shandon, Waltham, MA, US) using the Gene Expression Wash Buffer Kit (Agilent Technologies, Santa Clara, CA, US) according to the manufacturer's instructions. Slides were scanned using an Agilent Microarray Scanner (Agilent Technologies, Santa Clara, CA, US) with the default settings. Data were extracted with Feature Extraction Software 10.7 (Agilent Technologies, Santa Clara, CA, US) at the Biotechnology Corporation, Shanghai, PR China. Raw data were normalized using the Quantile algorithm in GeneSpring 11.0 (Agilent Technologies, Santa Clara, CA, US), and we considered genes that were up- or down-regulated by more than 1.5-fold in two independent biological duplicates.

IL-11 ELISA. IL-11 levels in normal culture medium collected after 48 h from different cells were detected with the Human IL-11 ELISA Kit (ab189569; Abcam, CA, USA) according to the manufacturer's instructions.

Statistical analysis. Statistical analyses were performed using SPSS 18.0 and GraphPad Prism 5.0. Numerical data are presented as the mean and standard error. Differences between proportions were evaluated using the paired Student's *t*-test. The correlations between TMED3 expression and clinicopathologic parameters were evaluated using chi-square tests, and survival analyses were evaluated by Kaplan–Meier analysis. *P* values ≤ 0.05 were considered statistically significant. Each experiment was repeated at least three times.

Data and materials availability. The microarray datasets have been deposited in the Gene Expression Omnibus (GEO) under GSE88772 (<https://www.ncbi.nlm.nih.gov/geo/query/acc.cgi?acc=GSE88772>).

References

1. Fan, S. T. *et al.* Continuous improvement of survival outcomes of resection of hepatocellular carcinoma: a 20-year experience. *Ann. Surg.* **253**, 745–758 (2011).
2. Rahbari, N. N. *et al.* Hepatocellular carcinoma: current management and perspectives for the future. *Ann. Surg.* **253**, 453–469 (2011).
3. Torre, L. A. *et al.* Global cancer statistics. *CA Cancer J. Clin.* **65**, 87–108 (2015).
4. Zhou, H. Y., Luo, Y., Chen, W. D. & Gong, G. Z. Hepatitis B virus mutation may play a role in hepatocellular carcinoma recurrence: A systematic review and meta-regression analysis. *J. Gastroenterol. Hepatol.* **30**, 977–983 (2015).
5. Cheung, Y. S. *et al.* Elevated perioperative transaminase level predicts intrahepatic recurrence in hepatitis B-related hepatocellular carcinoma after curative hepatectomy. *Asian J. Surg.* **31**, 41–49 (2008).

6. Wong, J. *et al.* Radiofrequency ablation for 110 malignant liver tumours: preliminary results on percutaneous and surgical approaches. *Asian J. Surg.* **32**, 13–20 (2009).
7. Wong, G. L. *et al.* Surveillance programme for hepatocellular carcinoma improves the survival of patients with chronic viral hepatitis. *Liver Int.* **28**, 79–87 (2008).
8. Kobayashi, T., Ishiyama, K. & Ohdan, H. Prevention of recurrence after curative treatment for hepatocellular carcinoma. *Surg. Today* **43**, 1347–1354 (2013).
9. Llovet, J. M., Fuster, J. & Bruix, J. Intention-to-treat analysis of surgical treatment for early hepatocellular carcinoma: resection versus transplantation. *Hepatology* **30**, 1434–1440 (1999).
10. Ryu, S. H. *et al.* Metastatic tumor antigen in hepatocellular carcinoma: golden roads toward personalized medicine. *Cancer Metastasis Rev.* **33**, 965–980 (2014).
11. Strating, J. R. & Martens, G. J. The p24 family and selective transport processes at the ER–Golgi interface. *Biol. Cell* **101**, 495–509 (2009).
12. Jerome-Majewska, L. A. *et al.* The trafficking protein Tmed2/p24beta(1) is required for morphogenesis of the mouse embryo and placenta. *Dev. Biol.* **341**, 154–166 (2010).
13. Carney, G. E. & Bowen, N. J. p24 proteins, intracellular trafficking, and behavior: *Drosophila melanogaster* provides insights and opportunities. *Biol. Cell* **96**, 271–278 (2004).
14. Jenne, N., Frey, K., Brugger, B. & Wieland, F. T. Oligomeric state and stoichiometry of p24 proteins in the early secretory pathway. *J. Biol. Chem.* **277**, 46504–46511 (2002).
15. Luo, W., Wang, Y. & Reiser, G. p24A, a type I transmembrane protein, controls ARF1-dependent resensitization of protease-activated receptor-2 by influence on receptor trafficking. *J. Biol. Chem.* **282**, 30246–30255 (2007).
16. Pastor-Cantizano, N. *et al.* p24 family proteins: key players in the regulation of trafficking along the secretory pathway. *Protoplasma* **253**, 967–985 (2016).
17. Connolly, D. J., O'Neill, L. A. & McGettrick, A. F. The gold domain-containing protein TMED1 is involved in interleukin-33 signaling. *J. Biol. Chem.* **288**, 5616–5623 (2013).
18. Doyle, S. L. *et al.* The gold domain-containing protein TMED7 inhibits TLR4 signalling from the endosome upon LPS stimulation. *Nat. Commun.* **3**, 707 (2012).
19. Liaunardy-Jopeace, A., Bryant, C. E. & Gay, N. J. The COP II adaptor protein TMED7 is required to initiate and mediate the delivery of TLR4 to the plasma membrane. *Sci. Signal.* **7**, ra70 (2014).
20. Palsson-McDermott, E. M. *et al.* TAG, a splice variant of the adaptor TRAM, negatively regulates the adaptor MyD88-independent TLR4 pathway. *Nat. Immunol.* **10**, 579–586 (2009).
21. Calon, A. *et al.* Dependency of colorectal cancer on a TGF- β -driven program in stromal cells for metastasis initiation. *Cancer Cell* **22**, 571–584 (2012).
22. Yuan, J. H. *et al.* A long noncoding RNA activated by TGF- β promotes the invasion-metastasis cascade in hepatocellular carcinoma. *Cancer Cell* **25**, 666–681 (2014).
23. Farazi, P. A. & DePinho, R. A. Hepatocellular carcinoma pathogenesis: from genes to environment. *Nat. Rev. Cancer* **6**, 674–687 (2006).
24. Chen, W. T. *et al.* Recurrent hepatocellular carcinoma after hepatic resection: prognostic factors and long-term outcome. *Eur. J. Surg. Oncol.* **30**, 414–420 (2004).
25. Shah, S. A. *et al.* Recurrence after liver resection for hepatocellular carcinoma: risk factors, treatment, and outcomes. *Surgery* **141**, 330–339 (2007).
26. You, A. *et al.* Metformin sensitizes sorafenib to inhibit postoperative recurrence and metastasis of hepatocellular carcinoma in orthotopic mouse models. *J. Hematol. Oncol.* **9**, 20 (2016).
27. Qi, L. N. *et al.* The p53 mutation spectrum in hepatocellular carcinoma from Guangxi, China: role of chronic hepatitis B virus infection and aflatoxin B1 exposure. *Liver Int.* **35**, 999–1009 (2015).
28. Ye, H. *et al.* Synergistic function of Kras mutation and HBx in initiation and progression of hepatocellular carcinoma in mice. *Oncogene* **33**, 5133–5138 (2014).
29. Hu, T. H. *et al.* Down-regulation of tumor suppressor gene PTEN, overexpression of p53, plus high proliferating cell nuclear antigen index predict poor patient outcome of hepatocellular carcinoma after resection. *Oncol. Rep.* **18**, 1417–1426 (2007).
30. Gao, J., Li, J., DU, J. & Li, X. Long non-coding RNA HOTAIR is a marker for hepatocellular carcinoma progression and tumor recurrence. *Oncol. Lett.* **11**, 1791–1798 (2016).
31. Chen, J. *et al.* The microtubule-associated protein PRC1 promotes early recurrence of hepatocellular carcinoma in association with the Wnt/ β -catenin signalling pathway. *Gut* (2016).
32. Duquet, A. *et al.* A novel genome-wide *in vivo* screen for metastatic suppressors in human colon cancer identifies the positive WNT–TCF pathway modulators TMED3 and SOX12. *EMBO Mol. Med.* **6**, 882–901 (2014).
33. Jarnicki, A., Putoczki, T. & Ernst, M. Stat3: linking inflammation to epithelial cancer - more than a “gut” feeling? *Cell Div.* **5**, 14 (2010).
34. Ernst, M. & Jenkins, B. J. Acquiring signalling specificity from the cytokine receptor gp130. *Trends Genet.* **20**, 23–32 (2004).
35. Ernst, M. & Putoczki, T. L. Molecular pathways: IL11 as a tumor-promoting cytokine-translational implications for cancers. *Clin. Cancer Res.* **20**, 5579–5588 (2014).
36. Putoczki, T. & Ernst, M. More than a sidekick: the IL-6 family cytokine IL-11 links inflammation to cancer. *J. Leukoc. Biol.* **88**, 1109–1117 (2010).
37. Putoczki, T. L. & Ernst, M. IL-11 signaling as a therapeutic target for cancer. *Immunother.* **7**, 441–453 (2015).
38. Hanavadi, S. *et al.* Expression of interleukin 11 and its receptor and their prognostic value in human breast cancer. *Ann. Surg. Oncol.* **13**, 802–808 (2006).
39. Yoshizaki, A. *et al.* Expression of interleukin (IL)-11 and IL-11 receptor in human colorectal adenocarcinoma: il-11 up-regulation of the invasive and proliferative activity of human colorectal carcinoma cells. *Int. J. Oncol.* **29**, 869–876 (2006).
40. Xiang, Z. L. *et al.* Potential prognostic biomarkers for bone metastasis from hepatocellular carcinoma. *Oncologist* **16**, 1028–1039 (2011).
41. Gurzov, E. N. *et al.* The JAK-STAT pathway in obesity and diabetes. *FEBS J.* doi: 10.1111/febs.13709 (2016).
42. Stark, G. R. & Darnell, J. E. The JAK-STAT pathway at twenty. *Immunity* **36**, 503–514 (2012).
43. Yang, S. *et al.* Activating JAK1 mutation may predict the sensitivity of JAK-STAT inhibition in hepatocellular carcinoma. *Oncotarget* **7**, 5461–5469 (2016).
44. Idris, N. M. *et al.* Activation of IL-11/STAT3 pathway in preconditioned human skeletal myoblasts blocks apoptotic cascade under oxidant stress. *Regen. Med.* **7**, 47–57 (2012).

Acknowledgements

The authors thank Shanghai Yuan Zhi Biological Technology Co., Ltd., and Shanghai Biotechnology Corporation, Ltd., for technical assistance. This study was supported by the National “973” Project of China (2014CB542102), the Science Fund for Creative Research Groups, the National Natural Science Foundation of China (NSFC; Grant Nos 81521091, 31370196, 81071681, 81171935, 81372207), the Shanghai Municipal Natural Science Foundation (132R1430800) and the Shanghai New Excellent Youth Plan (XYQ2013074).

Author Contributions

W.P.Z., H.R. and L.J.M. conceived the study and designed the experiments. W.P.Z. and L.J.M. provided the experimental materials. H.Z., Y.Y. and J.H. performed the experiments with the help of R.G., S.L., T.T., J.W., H.Z., C.C. and M.C.W. performed the data analysis. W.H.J., H.Z. and W.P.Z. wrote the manuscript. All authors contributed to the interpretation and discussion of the results, and reviewed the manuscript.

Additional Information

Supplementary information accompanies this paper at <http://www.nature.com/srep>

Competing financial interests: The authors declare no competing financial interests.

How to cite this article: Zheng, H. *et al.* TMED3 promotes hepatocellular carcinoma progression via IL-11/STAT3 signaling. *Sci. Rep.* **6**, 37070; doi: 10.1038/srep37070 (2016).

Publisher's note: Springer Nature remains neutral with regard to jurisdictional claims in published maps and institutional affiliations.



This work is licensed under a Creative Commons Attribution 4.0 International License. The images or other third party material in this article are included in the article's Creative Commons license, unless indicated otherwise in the credit line; if the material is not included under the Creative Commons license, users will need to obtain permission from the license holder to reproduce the material. To view a copy of this license, visit <http://creativecommons.org/licenses/by/4.0/>

© The Author(s) 2016